Capo: Calibrating Device-to-Device Positioning With a Collaborative Network

Kao Wan[1], Zhaoxi Wu[1], Qian Cao[2], Xiaotao Zheng[1], Ziwei Li[3], and Tong Li[4(✉)]

[1] Peng Cheng Laboratory, Shenzhen, China
[2] Xi'an University of Posts and Telecommunications, Xi'an, China
[3] Tsinghua University, Beijing, China
[4] Renmin University of China, Beijing, China
tong.li@ruc.edu.cn

Abstract. Device-to-device relative positioning has been widely applied in modern Web-based systems such as COVID-19 mobile contact tracing, seamless access systems, mobile interactive gaming, and mobile e-Commerce. The legacy absolute positioning technologies are not suitable for device-to-device positioning attributed to their mobility and heterogeneity of devices. In this paper, we focus on the heterogeneity problem and propose Capo, the first calibration algorithm that enables the interaction among devices with different communication modes for relative positioning in heterogeneous systems. Capo optimizes the ranging results of low-precision devices in a collaborative network based on the ranging data from high-precision devices. The evaluation shows that Capo can significantly improve up to 26.56% of the positioning accuracy of the heterogeneous systems. Real use case study on COVID-19 contact tracing further shows that Capo significantly improves the accuracy of exposure notifications.

Keywords: Relative positioning · Heterogeneous devices · Web based tracing.

1 Introduction

With the emergence of mobile devices and cloud computing, novel Web-based applications such as COVID-19 contact tracing [17], seamless access systems, mobile interactive gaming, robot navigation, and mobile e-Commerce have been widely promoted. The applications of mobile devices first collect positioning data and then interact with each other by connecting the cloud servers with Web services (e.g., HTTP, XML). The user experience is closely related to the precision of device-to-device positioning, the prerequisite stage of these applications.

Device-to-device positioning is a process by which mobile devices, such as smartphones or tablets, can determine their relative positions to one another without the use of external infrastructure like GPS. This is done through the exchange of wireless signals, which can be used to calculate the distances between

devices and then be used to infer their relative positions. For example, Apple recently released Airtag [12] portable hardware to provide users with fast and accurate tracking and positioning through Ultra-Wide Band (UWB). The proposal of such positioning methods also provides new ideas for the development direction of motion-sensing mobile games such as Nintendo Switch, a game console that supports Bluetooth Low Energy (BLE) to connect its controller to play motion-sensing games. Nintendo Switch has reached 125 million units worldwide in 2023 and this number will continue to increase. This indicates the immense potential values for the device-to-device relative positioning systems.

Although many schemes [4, 14, 16] for object positioning using pre-deployed anchors have been proposed, they mostly focus on absolute object positioning. They are not suitable for device-to-device relative positioning because of the mobility and heterogeneity of devices. First, due to the mobility of devices, a large number of devices may continue to join or withdraw from the positioning system, and it might be impossible to pre-deploy a number of fixed anchors in all the spots. Second, devices with different modes cannot communicate with each other. For example, a UWB-only device cannot parse a message from a BLE-only device. Due to the heterogeneity of devices, the legacy positioning systems mainly focused on the interaction between devices with the same communication mode, the positioning accuracy is therefore decided by the lower bound achieved by the most compatible mode among a group of devices. In this case, the precision of device-to-device positioning is decided by the BLE-based technology, although some of the devices support the UWB-based technology with higher accuracy [3].

Modern UWB technology is a pulse communication technology that started in the 1960s. However, UWB is a kind of new communication mode for mobile devices compared with the widely-deployed modes such as Wi-Fi, Bluetooth, etc. Recently, several companies have been developing UWB chips and antenna manufacturers to provide out-of-the-box solutions, but most of them only sell chips or demo kits rather than consumer-oriented products. When revisiting the evolution of Near-field communication (NFC) in the past two decades [10], we can easily infer that it takes a long time for a new mode to be supported by most devices. We thus believe that UWB-based positioning technology will have to coexist with legacy positioning technologies in the next few decades. Generally, it will be a significant contribution if we find a way to use a "high-precision mode" (e.g., UWB) to calibrate the device-to-device positioning of a "low-precision mode" (e.g., BLE).

In this paper, we propose Capo [18], an algorithm that improves the accuracy of low-precision device-to-device positioning with the help of high-precision ones. To the best of our knowledge, Capo is the first calibration algorithm that enables the interaction among devices with different communication modes for relative positioning in heterogeneous systems. In particular, Capo optimizes the ranging results of low-precision devices in a collaborative network based on the ranging data from high-precision devices. First, it calculates the actual distance from the high-precision device to the target low-precision device. Then it calculates the standard deviation of the distribution according to the signal attenuation

model and takes the actual distance as the mean to obtain the simulated ranging distance. Finally, the estimated coordinates of the target low-precision device are obtained by the least squares method, which greatly accurately locates the low-precision device. The evaluation shows that Capo can significantly improve $11.56\% \sim 26.56\%$ of the positioning accuracy of the system.

The remainder of this paper is organized as follows. Section 2 discusses the background and motivation of the paper. Section 3 introduces the overall design of the scheme. Section 4 presents the performance evaluation and studies a real-world use case of COVID-19 contact tracing. Finally, concluding remarks are made in Section 5.

2 Background and Motivation

Device-to-Device positioning requires high accuracy. Nowadays, there are many device-to-device applications, such as indoor navigation, and robotics that require centimeter-level high-precision positioning. However, only achieve meter-level positioning would lead to serious errors or even unavailability when running the application. Apple and Google have jointly proposed the Exposure Notification framework [1] in 2020 to help governments and public health authorities reduce the spread of COVID-19 through contact tracing applications. To improve framework capabilities, Huawei developed Contact Shield [2] to provide basic contact tracing services to detect the user's contact level with COVID-19 patients, ensuring the interoperability between Huawei phones and other Android/iOS phones.

Accuracy varies with different communication modes. Most works developing BLE-based [5] location systems use RSSI [11] to estimate location. And it was demonstrated that a scheme [7] using BLE as a location sensing medium is able to obtain 92% precision to within meters m accuracy. The positioning accuracy of the Wi-Fi signal-based positioning method [15] is in the range of 2-10 meters, and it has a serious problem of co-frequency interference. Aparicio et al. proposed a fusion method of BLE and Wi-Fi technologies for indoor positioning, which improved accuracy by 50 centimeters on average compared with the Wi-Fi positioning method. Due to the precision positioning potential of UWB technology with a centimeter scale and higher precision, it is the first choice for indoor high-precision positioning.

Low-precision devices can be enhanced by high-precision ones. Some interactions between high-precision devices and low-precision device, would have the potential to achieve better device-to-device positioning performance [13]. As shown in Figure 1(a), from the perspective of device O, it adopts BLE to compute the distances (OA, OB, OC) to the devices A, B, and C, with an error denoted by an arc-shaped shaded region. From the perspective of devices A, B, and C, they adopt UWB to compute the distances (AB, AC, BC) between each other. As shown in Figure 1(b), the relative positions of devices A, B, and C form a triangle. According to the constraint that devices A and C cannot be out of the scope of their shaded regions, we can infer that there might exist an unavailable location of device B in Figure 1(b) when the triangle moves to a

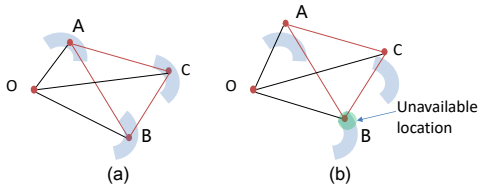

Fig. 1. Calibrating low-precision device using high-precision devices.

certain position. The relative position of the three high-precision devices adds a new position constraint to the ranging results of the low-precision devices, so as to narrow the margin of error of the low-precision devices.

3 The Capo Design

3.1 Design Rationale

Our goal is to calibrate device-to-device relative positioning for low-precision devices. To enable multiple high-precision devices to help the low-precision device in a collaborative network, inspired by the legacy absolute positioning technologies such as trilateral positioning, we give the design rationale of new solution. Theoretically, with only two high-precision devices, it might also be possible to enhance the position capability the low-precision devices, as detailed in section 3.3). For ease of understanding and description, we mainly consider the situation of at least three high-precision devices. In this case, the calibration of low-precision can be achieved in four steps. In step 1, we measure the relative positions between high-precision devices via the high-precision communication mode and initialize the coordinates of all high-precision devices. In step 2, we measure the distances (D1) between the low-precision device and the high-precision device via the low-precision communication mode. In step 3, a trilateral positioning algorithm can be used to locate the coordinates of the low-precision device. In step 4, recalculate the distances (D2) between the low-precision device and the high-precision device via the measured coordinates of the low-precision device. The distance set of D2 is regarded as the calibration of D1.

Assume three high-precision devices A, B, and C, and one target low-precision device O that are non-collinear on the plane. For each ranging device, we regard its coordinates as the center of the circle and the distance to point O as the radius, then we obtain three circles. Ideally, the three circles intersect at one point, which is the coordinate of the target device O. Since the measurement variation is ubiquitous, it may result in these circles to intersect in an area or even not intersect. Based on the above analysis, we propose a new positioning algorithm Capo to calculate the coordinates of the target point. Capo adopts the least squares method to solve the approximate coordinates of the target, which is detailed in the next section.

3.2 The Capo Algorithm

Capo assumes the ranging of low-precision communication mode based on RSSI obeys Gaussian distribution. The simplified model [6]of wireless signal attenua-

tion can be expressed as $RSSI_i = K_{\mathrm{dB}} - 10\gamma \log_{10}(d_i)$, where $RSSI_i$ signifies the received signal strength of i^{th} receiving end, and K_{dB} signifies the signal strength at a certain fixed distance from the signal source. For calculation convenience, this value is usually 1 meter [6].

Thus the ranging data can be generated based on the $RSSI_i$ equation mentioned above, γ represents the power falloff exponent, which is measured in practical applications and determined by the device type and its ranging accuracy. The lower the accuracy, the higher the value, and the greater the margin of error caused by the distance. If not specified, we set $\gamma = 5$. d_i represents the distance of the target away from the i^{th} signal source.

According to [8], the relation of the distance d and the signal strength can be displayed as $(d = 10^{\wedge} \frac{K_{dB} - RSSI_i}{10*\gamma})$. Therefore, the signal value conforming to the signal attenuation model can be used to express the error caused by the signal strength at a certain point. Since a large number of experiments have shown that the signal strength of RSSI at a certain point conforms to the Gaussian distribution [9] as the form of $RSSI \sim N\left(\mu, \sigma^2\right)$, where $\mu = \frac{1}{m}\sum_{i=1}^{m} RSSI_i$, and $\sigma^2 = \frac{1}{(m-1)}\sum_{i}^{m}\left(RSSI_i - \mu\right)^2$, so we can construct the ranging data distance values d that obey the distribution through the above-mentioned signal attenuation model based on the $RSSI_i$ equation. Algorithm 1 demonstrates the process of generating ranging data d.

Algorithm 1 Ranging data generation

Input: Set of points of high-precision devices P, P_i represents the i^{th} device $P_i(x_x.y_i)$. Measurement point $P_m(x_m, y_m)$. Power falloff exponent γ.

Output: Ranging data array d, d_i represents the ranging data obtained from i^{th} device.

$n \leftarrow 1$
$\sigma, error, distance \leftarrow 0$
while $n \leq i$ **do**
  $distance \leftarrow \sqrt{(x_n - x_m)^2 + (y_n - y_m)^2}$
  $\sigma \leftarrow \gamma * \log_{10}(distance)$
  $error \leftarrow$ Random number that follow the distribution $N(distance, \sigma^2)$
  $d_n \leftarrow distance + error$
end while
send d

Algorithm 2 The Capo

Input: A:i*2 matrix, B:i*1 matrix Ranging data array d, d_i represents the ranging data obtained from i^{th} device Set of points of high-precision devices P, P_i represents the i^{th} device $P_i(x_x.y_i)$.

Output: X, the 2*1 matrix.

$n \leftarrow 1$
while $n \leq i$ **do**
  if $n = 1$ **then**
    $A_{11} \leftarrow 2(x_1 - x_i)$, $A_{12} \leftarrow 2(y_1 - y_i)$
    $B_1 \leftarrow x_1^2 - x_i^2 + y_1^2 - y_i^2 + d_i^2 - d_1^2$
  else
    $A_{n1} \leftarrow 2(x_{n-1} - x_n)$, $A_{n2} \leftarrow 2(y_{n-1} - y_n)$
    $B_n \leftarrow x_{n-1}^2 - x_n^2 + y_{n-1}^2 - y_n^2 + d_n^2 - d_{n-1}^2$
  end if
end while
$X \leftarrow (A^T A)^{-1} A^T B$
send X

To apply the least squares method to solve the approximate solution based on the ranging results, we first establish the system of equations using the information from each device. Each equation within this system is in the form of: $(x_i - x)^2 + (y_i - y)^2 = d_i^2$, where x_i, y_i as the coordinates of the i^{th} device obtained via the high-precision positioning technology[5]. Then we calculate the

[5] Since the centimeter-level error of high precision technology is negligible compared to the meter-level error of low precision technology, for the sake of simplicity, in

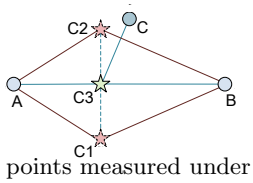

Fig. 2. Approximate target points measured under two high-precision devices.

non-linear equations to obtain the linear equations. Algorithm 2 demonstrates the process of applying the least squares method by ranging data d to obtain the approximate coordinate of the target device.

Finally, we use the least squares method to solve the above equations and obtain a two-dimensional column vector $X^T = [x\ y]$, representing the approximate coordinate (x, y) of the target point we obtained.

3.3 Discussion: Two High-precision Devices

We now discuss the effects of our algorithm for calibrating the coordinates of low-precision devices when there are only two high-precision devices. As shown in Figure 2, when there are only two high-precision devices A and B in the two-dimensional space, in theory, there should be two feasible point coordinates of device C, i.e., nodes C1 and C2. However, the actual output of the least squares method is node C3 instead. As illustrated in Figure 2, the ranging error between C3 and C might be much larger than that between C2 and C. In other words, applying Capo to a scenario with only two high-precision devices could potentially introduce extra biases.

The challenge here is that by applying the least squares method, we can only obtain a single approximate coordinate of the target point other than two. Thus, we infer that by adding a module of angle measurements, it is possible to indirectly compute the coordinates of C1 or C2 via the cosine function. However, we leave this for future work.

4 Evaluation

In this section, we first evaluate the overall performance of Capo with three high-precision devices. We then explore how Capo performs with different impact factors, such as a number of high-precision devices. We also investigate the extra overhead introduced by applying Capo. Finally, we give a case study of contact tracing, to further show the improvement of Capo in real-world scenarios.

4.1 Overall performance of Capo

For simplicity, we consider a heterogeneous system with three high-precision devices and one low-precision device in two-dimensional space. In this section,

this paper we assume a zero positioning error between high-precision devices, and d_i represents the ranging distance generated using the signal attenuation model mentioned above. These coordinates are The case of non-zero positioning error, however, we leave it as future work.

we conduct a simulation evaluation of the calibration performance of Capo, where three high-precision devices help the low-precision device achieve higher precision of device-to-device positioning. In practical implementation, we need the relative position of high-precision devices to conduct the calibration process. For these high-precision devices, the existing positioning methods (based on ToA, AoA, etc.) can be used to establish the relative coordinate relationship based on these high-precision devices. Since the calibration performance is independent of the absolute position of the devices, our experiment does not lose the general setting of the coordinates of the devices. The fixed coordinates of the three high-precision devices A, B and C are (-50,0), (10,40) and (20, -30) respectively, and the coordinates of low-precision ranging target device O are (5,5) (if not specified, the coordinate units are in meters). Noted that the coordinates of high-precision devices here are only for generating simulated ranging data, and absolute coordinates are not necessary for the practical implementation of Capo. The tests are conducted 3,000 times to explore the error distribution of the ranging results between the low-precision and high-precision devices.

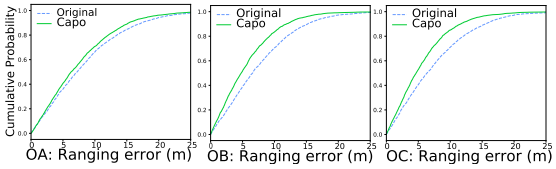

Fig. 3. Error distribution of the ranging result between device O and device A, B, C.

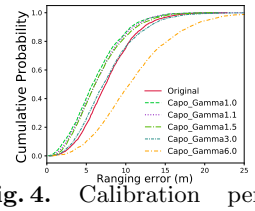

Fig. 4. Calibration performance of Capo in different γ values.

Figure 3 illustrates the calibration performance of Capo compared with the original way, which simply applies the wireless signal attenuation model. It is demonstrated that Capo can significantly calibrate the device-to-device positioning compared with the original way. Specifically, Capo improves the accuracy of the ranging between O and A by 11.56%, with the median ranging error decreasing from 6.9960 m to 6.1873 m. Similarly, it improves the ranging accuracy between O and B, and C by 24.76%, and 26.56%, respectively, leading to median ranging error reductions from 6.3081 m to 4.7461 m for O and B, and from 6.4972 m to 4.7715 m for O and C.

We further consider Capo's performance in the above scenario when the high-precision device has ranging errors in different γ values. The generation of high-precision device error values is also based on section 3.2. Since Capo does not give a specific positioning algorithm for high-precision devices, when simulating the high-precision device error in this scenario, the coordinate offset of the high-precision device caused by ranging error will be simulated by using the error generated from section 3.2. In particular, in this scenario, the algorithm employs the average distance among three high-precision devices for calculations.

Figure 4 illustrates the Capo's calibration performance when a high-precision device has ranging errors caused by different γ values compared with the original way (with γ being 1). It is demonstrated that when the high-precision device has

a relatively small γ compared to the low-precision device, Capo maintains stable calibration performance even considering the error in high-precision devices.

To summarize, the positioning results obtained by the Capo algorithm have an optimization effect on each device in the system, which can improve the accuracy of the positioning results as a whole. This relies on Capo making full use of three high-precision devices to provide more calibration data for the ranging of the low-precision device.

4.2 Overhead analysis of Capo

We further evaluate the communication overhead of running Capo among devices. We let C_h and C_l denote the ranging cost required by the high-precision device and the low-precision device respectively, noting that $C_h = 2C_l$. And assume n is the number of high-precision devices. We define the overhead of the system running Capo as follows: $\text{Cost} = n^*(n-1)^*C_h + n^*C_l$.

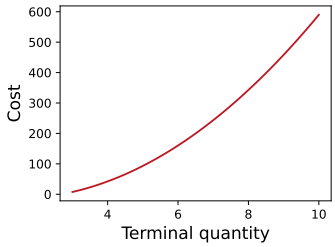

Fig. 5. Overhead of Capo with the number of high-precision devices.

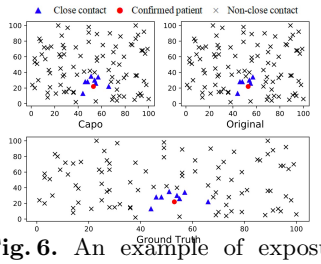

Fig. 6. An example of exposure check results.

Figure 5 demonstrates that the cost of Capo rises with an increase in the number of devices, attributed to the heightened number of interactions leading to higher overhead. However, we believe the improved ranging accuracy will more than pay for the Capo overhead if we limit the maximum number of high-precision devices N_{max}, for instance, $N_{max} = 4$.

Based on the above observations, we find that 4 high-precision devices gain a considerable accuracy improvement with a slightly increased cost compared with 2, 3, 5, and 6 high-precision devices. We infer that the inclusion of a fourth high-precision device, if feasible, has the potential to substantially enhance the overall performance of the calibration system.

4.3 Case Study: Contact Tracing

We apply Capo in a COVID-19 Contact Tracing application to improve system-ranging performance for more accurate exposure notifications and Figure 6 shows an example of exposure check results. We take the 100 m $\times$ 100 m space as the experimental scene, where 100 users are randomly distributed. One confirmed patient was randomly selected for each test and the test was repeated 1,000 times. Note that since scenes with several confirmed patients can be divided into multiple independent scenes with a single confirmed patient, repeating a single experiment can restore the practical situation.

Methodology. We assume that the confirmed patient uses a BLE-only device (i.e., a low-precision device with $\gamma = 5$)[6], and other users use both UWB and BLE enabled devices (i.e., high-precision devices). The safe distance is regarded as 1 meter and by applying Capo, UWB ranging is used to assist in improving the ranging results of low-precision BLE devices. As concluded above, 4 high-precision devices are enough for calibration, and in this scenario, if there are more than four UWB devices in the scene, only 4 UWBs need to be selected to complete the calibration. After calibrating device-to-device ranging with Capo, a list of close contacts and non-close contacts is obtained by comparing the safe distance with the measured distance.

Performance evaluation metrics. For each test, we evaluate its accuracy, precision, and recall by calculating the classification results of Capo, Original (without Capo), and Ground Truth.

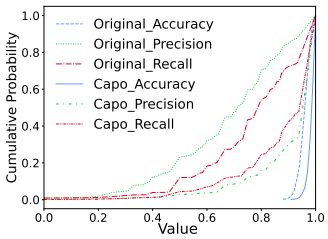

Fig. 7. Capo improves exposure notification in Contact Tracing system ($\gamma = 5$).

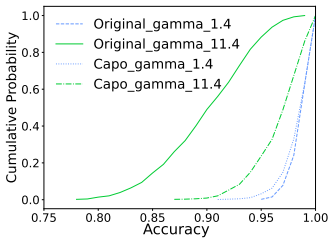

Fig. 8. Accuracy with different value of γ .

Results. The classification results of Capo and Original are illustrated in Figure 7. The accuracy of contact tracing classification using Capo is obviously higher than that using Original. Specifically, the application of Capo has resulted in an increase in accuracy by over 60%, elevating it from 95% to 98%, and his improvement is attributed to Capo's ability to calibrate device-to-device ranging among low-precision BLE devices using high-precision UWB devices.

We further explore the impact of varying values of γ, and Figure 8 shows that Capo's augmented benefit as γ increases. This reveals that the lower the precision of the device, the more benefit we can get by applying Capo.

5 Conclusion

In this paper, we proposed Capo for calibrating device-to-device positioning in heterogeneous systems. By applying Capo, the ranging accuracy of low-precision devices can be significantly improved according to the relative positioning of high-precision devices. Evaluation results further show that Capo with four high-precision devices can balance calibration performance and cost well, which is rec-

[6] According to the $RSSI_i$ equation, based on the scale of the distance and BLE's RSSI-based ranging error of 2–10 m, we set $\gamma = 5$ for BLE devices.

ommended. We studied a real-world use case of contact tracing, and the results show that Capo significantly improves the accuracy of exposure notifications.

Acknowledgements. This work is supported by NSFC Project (Grant No. 62202473, 62132011, 62132009), National Key R&D Program of China (Grant No. 2022YFB3105000), and PCL Future Regional Network Facilities for Large-scale Experiments and Applications (Grant No. PCL2018KP001).

References

1. Gaen. https://www.google.com/covid19/exposurenotifications (2022)
2. Huawei contact shield. https://developer.huawei.com/consumer/en/doc/development/system-Guides/contactshield-introduction-0000001057494465 (2022)
3. Chen, Y.C., Alexsander, I., Lai, C., Wu, R.B.: Uwb-assisted high-precision positioning in a utm prototype. In: 2020 IEEE WiSNeT. pp. 42–45 (2020)
4. Cheng, L., Wang, Y., Xue, M., Bi, Y.: An indoor robust localization algorithm based on data association technique. Sensors **20**(22), 6598 (2020)
5. Ding, Y., Li, T., Liang, J., Wang, D.: Blender: Toward practical simulation framework for ble neighbor discovery. In: MSWiM. pp. 103–110 (2022)
6. Durgin, G., Rappaport, T.S., Xu, H.: Measurements and models for radio path loss and penetration loss in and around homes and trees at 5.85 ghz. IEEE Transactions on communications **46**(11), 1484–1496 (1998)
7. Ho, Y.H., Chan, H.C.: Blueprint: Ble positioning algorithm based on nufo detection. In: 2017-2017 IEEE GLOBECOM. pp. 1–6 (2017)
8. Jayakody, J.A., Lokuliyana, S., Chathurangi, D., Vithana, D., et al.: Indoor positioning: Novel approach for bluetooth networks using rssi smoothing. International Journal of Computer Applications **137**(13), 26–32 (2016)
9. Jianyong, Z., Haiyong, L., Zili, C., Zhaohui, L.: Rssi based bluetooth low energy indoor positioning. In: IPIN. pp. 526–533 (2014)
10. Lazaro, A., Villarino, R., Girbau, D.: A survey of nfc sensors based on energy harvesting for iot applications. Sensors **18**(11), 3746 (2018)
11. Li, G., Geng, E., Ye, Z., Xu, Y., Lin, J., Pang, Y.: Indoor positioning algorithm based on the improved rssi distance model. Sensors **18**(9), 2820 (2018)
12. Li, T., Liang, J., Ding, Y., Zheng, K., Zhang, X., Xu, K.: On design and performance of offline finding network. In: IEEE INFOCOM. pp. 1–10 (2023)
13. Li, T., Zheng, K., Xu, K., Jadhav, R.A., Xiong, T., Winstein, K., Tan, K.: Tack: Improving wireless transport performance by taming acknowledgments. In: ACM SIGCOMM. pp. 15 – 30 (2020)
14. Li, Z., Xu, K., Wang, H., Zhao, Y., Wang, X., Shen, M.: Machine-learning-based positioning: A survey and future directions. IEEE Network **33**(3), 96–101 (2019)
15. Liu, F., Liu, J., Yin, Y., Wang, W., Hu, D., Chen, P., Niu, Q.: Survey on wifi-based indoor positioning techniques. IET communications **14**(9), 1372–1383 (2020)
16. Mayer, P., Magno, M., Schnetzler, C., Benini, L.: Embeduwb: Low power embedded high-precision and low latency uwb localization. In: WF-IoT. pp. 519–523 (2019)
17. Shen, M., Wei, Y., Li, T.: Bluetooth-based covid-19 proximity tracing proposals: An overview. arXiv2008.12469 (2020)
18. Wu, Z., Cao, Q., Zheng, X.: Capo's publication version with the implementation and experimental data(capo_rssp_python v2.1). zenodo. (Aug 2023), https://doi.org/10.5281/zenodo.8246597